Biochimica et Biophysica Acta 1838 (2014) 456–464

Contents lists available at ScienceDirect

Biochimica et Biophysica Acta

journal homepage: www.elsevier.com/locate/bbamem

Lipid bilayers containing sphingomyelins and ceramides of varying N-acyl lengths: A glimpse into sphingolipid complexity

Noemi Jiménez-Rojo, Aritz B. García-Arribas, Jesús Sot, Alicia Alonso, Félix M. Goñi *

Unidad de Biofísica (CSIC, UPV/EHU), Universidad del País Vasco, P.O. Box 644, 48080 Bilbao, Spain
Departamento de Bioquímica, Universidad del País Vasco, P.O. Box 644, 48080 Bilbao, Spain

ARTICLE INFO

Article history:
Received 22 July 2013
Received in revised form 9 October 2013
Accepted 11 October 2013
Available online 19 October 2013

Keywords:
Sphingomyelin
Ceramide
Differential scanning calorimetry
Atomic force microscopy
Sphingomyelinase
Interdigitation

ABSTRACT

The thermotropic properties of aqueous dispersions of sphingomyelins (SM) and ceramides (Cer) with N-acyl chains varying from C6:0 to C24:1, either pure or in binary mixtures, have been examined by differential scanning calorimetry. Even in the pure state, Cer and particularly SM exhibited complex endotherms, and their thermal properties did not vary in a predictable way with changes in structure. In some cases, e.g. C18:0 SM, atomic force microscopy revealed coexisting lamellar domains made of a single lipid. Partial chain interdigitation and metastable crystalline states were deemed responsible for the complex behavior. SM:Cer mixtures (90:10 mol ratio) gave rise to bilayers containing separate SM-rich and Cer-rich domains. In vesicles made of more complex mixtures (SM:PE:Chol, 2:1:1), it is known that sphingomyelinase degradation of SM to Cer is accompanied by vesicle aggregation and release of aqueous contents. These vesicles did not reveal observable domain separation by confocal microscopy. Vesicle aggregation occurred at a faster rate for those bilayers that appeared to be more fluid according to differential scanning calorimetry. Content efflux rates measured by fluorescence spectroscopy were highest with C18:0 and C18:1 SM, and in general those rates did not vary regularly with other physical properties of SM or Cer. In general the individual SM and Cer appear to have particular thermotropic properties, often unrelated to the changes in N-acyl chain.

1. Introduction

Research on sphingolipids, and in particular the structurally simplest among them, e.g. ceramides, sphingosine, is knowing a Golden Age because of the recognition of those lipids as bioactive molecules in the last two decades. Ceramides (Cer) have constituted an important field of research, from the points of view both of biology/biochemistry [1] and of biophysics [2]. Efforts have also been made to connect these two areas of study [3,4]. In their review, Hannun and Obeid [1] suggested that in mammals different synthetic pathways gave rise to over 200 structurally different Cer, and that distinct Cer molecular species would execute distinct functions in distinct subcellular compartments.

The purpose of the present study was to explore whether the physical properties of Cer, and of their related molecule sphingomyelins (SM), were relatively invariant within each lipid class, or else changed with the N-acyl chain, and, in the latter case, whether or not the change occurred in parallel with chain length and/or unsaturation. Samples containing pure SM, pure Cer, or mixtures, all in aqueous dispersions, have been examined.

Similar studies have been performed by other authors in which factors other than N-acyl chain length have been considered, such as sphingoid base length [5], or SM head group size in mixtures with palmitoyl Cer [6]. Pinto et al. [7] described in detail the biophysical properties of the long-chain, asymmetric C24:1 ceramide, both pure and in mixtures with 1-palmitoyl-2-oleoylphosphatidylcholine. More recently, the same authors have compared the properties of C16:0, C18:0, C18:1, C24:0 and C24:1 ceramides in mixtures with POPC, using fluorescence spectroscopy and microscopy [8]. Also Westerlund et al. [9] studied the thermotropic properties of mixtures of C16:0 SM with Cer of varying N-acyl chain lengths. In our study, both the properties of the individual molecules (Cer or SM, N-acyl chains from C6:0 to C24:1), and of mixtures in which N-acyl chain lengths of Cer and SM were independently varied, were studied.

SM:Cer mixtures are important because these two lipids have a mutual affinity, at least in the absence of cholesterol (Chol) [10,11], and because Cer is the lipidic end-product of SM hydrolysis by sphingomyelinase at the beginning of the sphingolipid signaling pathway [12]. For this reason we also assayed sphingomyelinase activity on vesicle containing SM with different N-acyl chains. Ceramide generation under these conditions leads to liposomal aggregation and release of vesicular aqueous contents [13,14]. Our studies of Cer and SM, either individually or in binary or in more complex mixtures, reveal an intricate map of biophysical properties that often do not follow recognizable patterns. Thus the biological, biochemical and chemical diversities of Cer discussed by Hannun and Obeid [1] are also accompanied by a heterogeneity of biophysical properties.

* Corresponding author. Fax.: +34 94 601 33 60.
E-mail address: felix.goni@ehu.es (F.M. Goñi).

0005-2736/$ – see front matter © 2013 Elsevier B.V. All rights reserved.
http://dx.doi.org/10.1016/j.bbamem.2013.10.010

2. Materials and methods

2.1. Materials

Sphingomyelinase (S7651) from *Bacillus cereus* was supplied by Sigma. Egg PE was purchased from Lipid Products (South Nutfield, UK). Fatty acid composition of egg PE was: 22% 16:0, 37.4% 18:0, 29.4% 18:1, 11.2 C18:2. All the sphingomyelins and ceramides were from Avanti Polar Lipids (Alabaster, AL). ANTS and DPX were supplied by Molecular Probes, Inc. (Eugene, OR).

2.2. Methods

2.2.1. Differential scanning calorimetry

All measurements were performed in a VP-DSC high-sensitivity scanning microcalorimeter (MicroCal, Northampton, MA). Both lipid and buffer solutions were fully degassed before loading into the appropriate cell. Buffer was 20 mM PIPES, 150 mM NaCl, 1 mM EDTA, pH 7.4. Lipid suspensions were loaded into the microcalorimeter in the form of multilamellar vesicles. For vesicle preparation the lipids were hydrated in buffer, with dispersion facilitated by stirring with a glass rod, and finally the solutions were extruded through a narrow tubing (0.5 mm internal diameter, 10 cm long) between two syringes 100 times at 75 °C, above the transition temperature of the SM-Cer mixtures. A final amount of 0.5 ml at 0.5 mM total lipid concentration was loaded into the calorimeter, and up to six heating scans were performed at 45 °C/h between 10 and 105 °C for all samples. Lipid concentration was determined as lipid phosphorus, and used together with data from the last scan, to obtain normalized thermograms. The software Origin 7.0 (MicroCal), provided with the calorimeter, was used to determine the different parameters for the scans. The software PeakFit v4.12 was used for curve-fitting. Third/fourth scans are shown in the Figs. 1, 4, and S1–S8.

2.2.2. Supported Planar Bilayer (SPB) preparation

SPBs were prepared on high V-2 quality scratch-free mica substrates (Asheville-Schoonmaker Mica Co., Newport News, VA) previously attached to round 24 mm glass coverslips by the use of a two-component optical epoxy resin (EPO-TEK 301-2FL, Epoxy Technology Inc., Billerica, MA). SPBs were prepared using the well-known vesicle adsorption method [15]. For this methodology, multilamellar vesicles (MLVs) were initially prepared by mixing the appropriate amount of synthetic pure sSM in chloroform/methanol (2:1, v/v) solutions, including 0.4 mol% DiI. Samples were then dried by evaporating the solvent under a stream of nitrogen and by placing them into high vacuum for 2 h. The samples were then hydrated in assay buffer and highly vortexed at a temperature above that of the sample lipids' highest phase transition. After complete lipid detachment from the bottom of the test tube, formed MLVs were introduced in an FB-15049 (Fisher Scientific Inc., Waltham, MA) bath sonicator and kept at 60 °C for 1 h. In this way a proportion of small unilamellar vesicles (SUVs) were generated. Thereafter, 120 μl of assay buffer containing 3 mM $CaCl_2$ were added onto previously prepared 1.2 cm^2 freshly cleaved mica substrate mounted onto a BioCell coverslip-based liquid cell for atomic force microscopy (AFM) measurements (JPK Instruments, Berlin, Germany). 60 μl sonicated vesicles were then added on top of the mica. Final lipid concentration was 150 μM. Vesicles were left to adsorb and extend for 30 min maintaining the sample temperature at 70 °C. Another 30 min were left for the samples to equilibrate at room temperature, discarding then the non-adsorbed vesicles by washing the samples 10 times with assay buffer in $CaCl_2$ absence. A small amount of buffer was always left on top of the substrate in order to maintain sSM SPBs hydrated at all times. The BioCell was set to 23 °C and the planar bilayers were left to equilibrate for 1 h prior to AFM measurements. After the completion of AFM images at 23 °C, the BioCell was set to 39 °C and SPBs were left to equilibrate for 45 min before being measured again by AFM imaging.

2.2.3. Atomic force microscopy

The measurements were performed on a NanoWizard II AFM (JPK Instruments) at 22 °C. MLCT SiN cantilevers (Veeco Instruments, Plainview, NY) with a spring constant of 0.1–0.5 N/m were used in contact mode scanning (constant vertical deflection) to measure the supported phospholipid bilayers (SPBs). Resolution images measuring 512 × 512 pixels were collected at a scanning rate of 1 Hz and line-fitted using the JPK Image Processing software as required, so that bilayer thickness could be accurately calculated by cross-section height analysis.

2.2.4. Enzyme activity

Sphingomyelinase activity was assayed by determining phosphorus contents [16]. Liposome concentration was 0.3 mM in all the experiments.

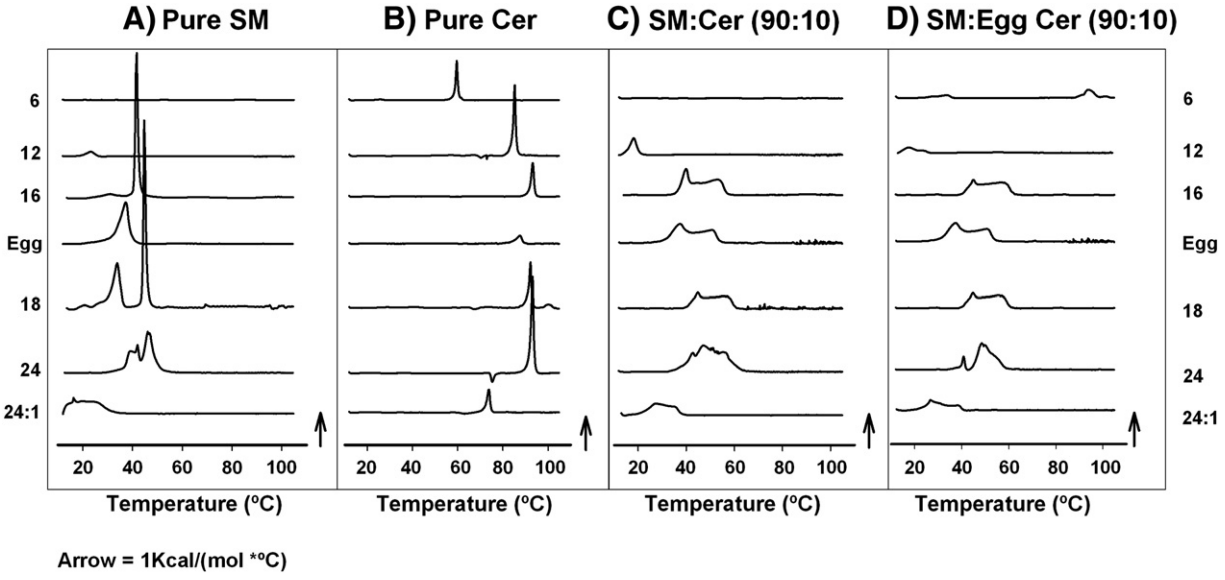

Fig. 1. DSC thermograms of pure sphingolipids and binary mixtures. Chain lengths are indicated by the sides of the figure. Representative results (3rd scans) of two very similar measurements. (A) Pure SM. (B) Pure Cer. (C) SM:Cer (90:10 mol ratio) mixtures, both SM and Cer with the same N-acyl chain. (D) SM:egg Cer (90:10 mol ratio) mixtures.

For optimal catalytic activity the enzyme was assayed at 37 °C, in 25 mM HEPES, 100 mM NaCl, pH 7.2. Enzyme concentration was 0.5 μg/ml. Enzyme activity was assayed by determining water-soluble phosphorus. Aliquots (50 μl) were removed from the reaction mixture at regular intervals and extracted with 250 μl of a chloroform/methanol/conc. hydrochloric acid mixture (66/33/1, v/v/v) and the aqueous phase was assayed for phosphorus contents.

2.2.5. Vesicle aggregation

Liposome aggregation was estimated as an increase in turbidity (absorbance at 400 nm) measured in a UV–Vis Cary 3 Bio (Varian Instruments) spectrophotometer. Lag times for the aggregation events were computed from the individual time course plots as the time at which the maximum slope line intersects with the '0% effect' base line.

2.2.6. Fluorescence spectroscopy

Vesicle efflux was usually assayed with the ANTS-DPX fluorescent system [17]. DPX forms a complex with and quenches fluorescence of ANTS. When both molecules are entrapped in a vesicle, ANTS fluorescence is low. When they are released to the surrounding aqueous medium, the complex dissociates, and ANTS fluorescence increases. Details on the use of these fluorescent probes, including assay calibration, are given elsewhere [18,19]. Fluorescence measurements were performed in an Aminco Bowman Series 2 luminescence spectrometer.

3. Results

3.1. Thermotropic properties of pure sphingomyelins

All SM tested, with 12, 16, 18, 24 and 24:1 N-acyl chains respectively, exhibited endothermic signals in the 10–100 °C range when studied in excess water by DSC. C6 SM however showed no thermotropic behavior in this temperature range. Representative thermograms are shown in Fig. 1A, and in more detail, in Figs. S1A–S7A. Data for egg SM, containing mostly (≈80%) N-acyl C16:0 are also included for comparison. Unlike the saturated phosphatidylcholines, that exhibit single, symmetrical DSC endotherms, the corresponding SM signals were complex and asymmetric, suggesting the presence of several, partially overlapping, transitions, with the possible exception of C16 SM. The thermodynamic parameters of the observed thermotropic transitions are summarized in Table 1. By analogy with previous studies, in which DSC data of SM have been performed in parallel with X-ray [20] or fluorescence spectroscopy [21] measurements, it can be concluded that the endotherms observed in Fig. 1A correspond to gel-fluid transitions of SM.

The midpoint transition temperatures T_m of SM with saturated N-acyl chains increase with chain length, although the increase is moderate above C16 (Table 1). Introduction of a *cis* double bond in the C24 chain causes a clear decrease in T_m, as commonly observed for the phosphatidylcholines. The transition enthalpies also increase with chain length (Table 1). These data suggest that C6 SM may have a transition with a feeble ΔH below the temperature range of our thermograms (<10 °C). Our observations are in agreement with partial data from other laboratories [20–23], some differences being attributed to the less sensitive instrumentation used in the older studies.

The fact that the endotherms become more complex and asymmetric as the N-acyl chain length deviates from C16 is interesting because in C16 SM in bilayer form the hydrophobic moieties of the sphingosine and N-acyl chains have about the same length. In the other cases, the larger the length difference between the sphingosine and the N-acyl chain, the more complex is the endothern. Asymmetric chain lengths are likely to give rise to partial interdigitation when the SM are forming bilayers, as suggested by previous authors [22,24]. Thus interdigitation appears to give rise, even in bilayers composed of a single SM, to different domains that are extensive enough to give rise to cooperative transitions detectable by DSC. This in turn suggests that partial interdigitation is not a phenomenon that occurs evenly along the plane of the bilayer. The phenomenon certainly deserves further investigation, particularly because very long chain sphingolipids are known to exist in nature [25,26]. Apart from chain length asymmetry, Shah et al. [27] suggested that the complex thermotropic behavior of sphingolipids was due, at least partly, to the complex H-bond network connecting the lipid headgroups in the bilayer.

Perhaps as another consequence of chain asymmetry, this time with a shorter N-acyl than sphingosine chain, C12 SM, either pure (Fig. S2A) or in mixtures with ceramides (Figs. S2B, S2C), gives rise to exceedingly wide (WHH > 15 °C), low-enthalpy signals (Tables 1, 3, 4) whose interpretation remains at present unknown.

Table 1
Thermodynamic parameters of thermotropic transitions of sphingomyelins. T_M of the main transitions are indicated in bold.

N-acyl chain	Components	T_m (°C)		ΔH (Kcal/mol)		WHH (°C)		
6		–				–		
12		23.4		0.96		4.0		
	1		21.1	0.22				4.9
	2		23.4	0.43				3.3
	3		54.9	0.15				16.6
	4		75.1	0.11				15.2
16		30.9	**41.7**	0.59	6.64	6.7	1.1	
Egg		38.1		6.86			3.4	
	1		33.6		2.08			11.8
	2		37.0		3.59			4.4
	3		38.1		1.18			1.6
18		33.9	**44.7**	5.2	7.6	3.4	1.1	
	1		31.1		2.06			5.8
	2		33.8		3.38			2.7
	3		44.9		6.85			1.1
24		46.1		10.4			10.1	
	1		38.8		1.94			5.7
	2		41.8		2.26			1.0
	3		46.4		4.41			3.4
	4		49.7		0.99			5.4
24:1		24.1		6.25			14.7	
	1		14.1		0.66			2.4
	2		16.4		0.27			1.4
	3		18.1		1.42			5.5
	4		24.3		3.85			9.7

3.2. Atomic force spectroscopy of C18:0 SM

The phenomenon of complex DSC signals in pure SM was studied in more details for the favorable case of C18.0 SM, in which two calorimetric signals, centered respectively at 33.9 and 44.7 °C, show baseline resolution under our conditions. Bilayers consisting of hydrated pure C18 SM were spread onto a mica plate and examined by AFM at 23 °C, 39 °C and 47 °C at apparently 0 Cp (Figs. 1A and S5A), i.e. respectively below the 33.9 °C transition, in the region between the two observed thermotropic transitions, and above the transitions. The results in Fig. 2A, B show (apart from the black regions that correspond to non-coated mica) a mostly brown surface of C18:0 SM at 23 °C, with small yellow specks. The continuous phase has an average height 7.32 ± 0.35 nm (n = 80, two independent preparations) The very small yellow (thick) spots could not be studied in detail. At 39 °C (Fig. 2C, D) two kinds of coexisting domains were observed, of heights 7.20 ± 0.25 nm (n = 50) and 5.25 ± 0.28 nm (n = 50) respectively (data obtained from two independent preparations). The difference in height between the continuous phase at 23 °C and the higher phase (yellow) at 39 °C is slightly significant ($p = 0.034$ according to Student's *t*-test). Our provisional interpretation is that at 39 °C a non-interdigitated gel phase (yellow) coexists with a partially interdigitated one (brown). No interdigitation would exist at 23 °C. Note that for the C18:0 SM at 39 °C, sample equilibration for ~45 min was required for

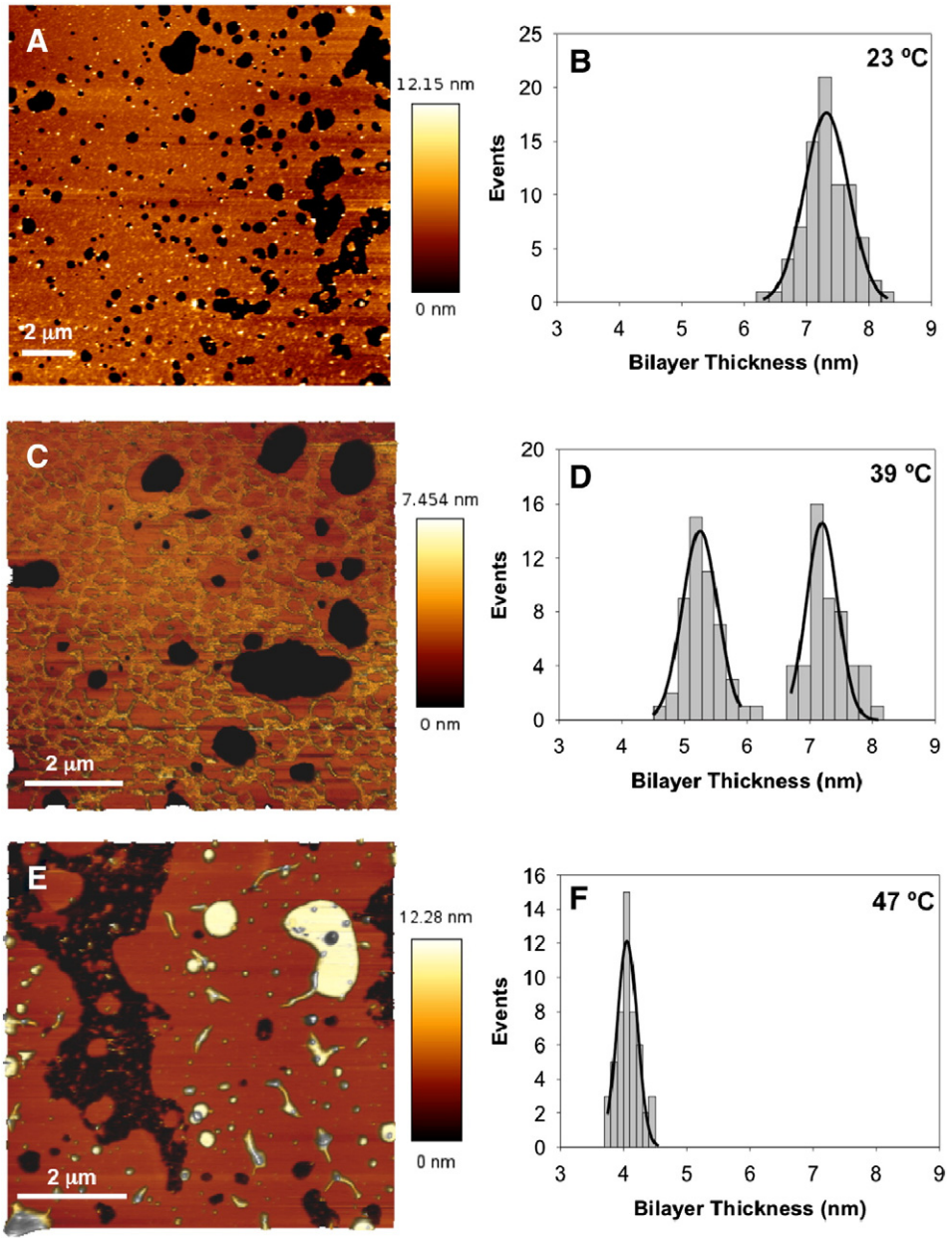

Fig. 2. AFM images and histograms of bilayer thickness measurements. Topographical AFM height images of C18:0 SM supported lipid bilayers at 23 °C (A), 39 °C (C) and 47 °C (E), with their respective histograms of bilayer thicknesses and Gaussian fittings (B, D, F). Bilayer thickness value obtained at 23 °C is 7.32 ± 0.35 nm. Measurements at 39 °C include data from both lipid phases that can be easily identified by their significantly different height (5.25 ± 0.28 nm and 7.20 ± 0.25 nm). Bilayer thickness value obtained at 47 °C is 4.06 ± 0.16 nm. Thickness measurements have been made by cross-section height analysis (n = 50–100) of the AFM images taken from two different samples.

domain separation to be visible. Under steady state conditions, the higher and lower phases covered areas in approximately a 1:2 ratio. The lower phase formed discontinuous domains within a continuous higher phase. The domains were very heterogeneous in size, from ~50 nm to about 1 μm. When, after equilibration at 39 °C, the sample was annealed to 23 °C, the heterogeneity was still visible for a time, the system showing hysteresis. Above the observed endotherms (47 °C) (Fig. 2E, F) a continuous fluid phase (4.03 ± 0.16 nm, n = 50 in two preparations) is seen (the white areas correspond to regions with two superimposed bilayers).

3.3. Thermotropic properties of pure ceramides

Water dispersions of egg ceramide and of chemically defined ceramides with N-acyl chains from C6 to C24:1 were examined by DSC. The thermograms are shown in Fig. 1B (in more detail in Fig. S8) and the corresponding thermodynamic parameters are summarized in Table 2.

Table 2
Thermodynamic parameters of thermotropic transitions of ceramides. T_M of the main transitions are indicated in bold.

N-acyl chain	T_m (°C)			ΔH (Kcal/mol)			WHH (°C)		
6	59.6			1.7			1.0		
12	70.3	**85.2**			−0.07	3.73	1.1		
16	93.2			2.24			1.4		
Egg	87.5			0.91			3.0		
18	67.5	**92.2**	99.9	−0.11	2.36	0.31	1.1	3.3	
24	75.3	**93.2**			−0.42	5.02			
24:1	63.1	**73.7**	81.7	0.16	1.46	0.03	4.1	1.6	0.9

In general ceramide thermograms were simpler than those arising from SM, and consisted of a main narrow endotherm, sometimes accompanied by small, wider endotherms, and even small exotherms. T_m of the main endotherm increased with chain length of the saturated species, up to C16:0, and ΔH also increased in a similar way. Smaller exotherms were found with the longer-chain ceramides, C18:0 and C24:0, that represented in both cases ~12–13% of the total heat absorbed. Small exotherms were also observed in several samples, at temperatures always below that of the main transition (Table 2). These exotherms were present even when the most painstaking efforts were made to achieve a homogeneous hydration, and did not show major changes when the sample was stored for up to 48 h at room temperature or at 4 °C before the measurements. These exotherms have been attributed [9,27] to metastable crystalline phases that change into more stable gel phases before melting.

Our T_m values for the main endotherms (Table 2, figures in bold) are in good agreement with those published by Shah et al. [26] and by Westerlund et al. [9]. However Pinto et al. [7] reported DSC data for C24:1 ceramide that are clearly different from ours. In their case the main endotherm was centered at ~52 °C, vs. ~74 °C in our case, the difference being probably due to sample preparation, that included in their case several freeze–thaw cycles, while in our method dispersion was facilitated by forcing the water/ceramide mixture through a narrow tubing, at high temperature. Many authors [9,27,28] in the past have pointed out the importance of the sample thermal history in Cer studies, and particularly for the long-chain ones.

3.4. Thermotropic properties of SM:Cer mixtures

Two series of experiments were performed, one in which SM (C6 to C24:1) were mixed at a 90:10 mol ratios with Cer containing the same N-acyl component. The mixture would reflect the properties of a system in which SM has been partially hydrolyzed to Cer and phosphorylcholine by a sphingomyelinase. The 90:10 ratio was selected as one in which, at least for the egg SM:egg Cer couple, the effects of Cer on the SM gel–fluid transition were clearly seen [6]. In a different series of preparations each SM was mixed with 10 mol% egg Cer, the latter representing a common natural ceramide. Thus our studies complement the data by Westerlund et al. [5] in which different ceramides (C4–C24:1) are mixed with C16 SM.

For mixtures containing identical N-acyl chains the thermograms can be seen in Fig. 1C, and the derived thermodynamic parameters, in Table 3. The thermograms can be seen in more detail in Figs. S1B–S7B. In general the SM:Cer mixtures give rise to transitions in a temperature range similar to that of the corresponding SM (compare Fig. 1A and C). Accordingly the C6SM: C6 Cer mixture shows no transition in the T range under study, in spite of the narrow endotherm of pure C6 ceramide. The endotherms are made broader in the mixtures, with no signs of pure Cer melting in the high-T region, indicating good mixing in all cases. The complex endotherms in Fig. 1C can be decomposed in a number of constituent transitions, as shown previously by us [10,29,30] and other authors [9], (see also Supplementary Figs. S1–S8). The complexity of the pure SM endotherms, particularly C18 and C24 (Fig. 1A) has been attributed to hydrocarbon chain interdigitation arising from lipid chain length asymmetry (see above). While asymmetry may still play a role in the generation of complex endotherms in C24 and C24:1 SM:Cer couples (note that the lineshapes in Fig. 1A and C are very similar for these mixtures) another factor must operate particularly in the C16 and C18 mixtures, that exhibit complex endotherms (Figs. S3B and S5B) with a small asymmetry. Interestingly, in these complex endotherms, there is always a relatively narrow component whose T_m is very close to that of the pure SM. This suggests that at the SM:Cer 90:10 mol ratio there remains a fraction of SM in domains that are poor in Cer. Thus partial unmixing would be an additional contributor to the observed signal complexity. We have recently shown, in a collaborative work with J. Thewalt, using ^2H NMR and alternating perdeuterated with proton-based N-acyl chains in C16:0 SM and C16:0 Cer, that SM and Cer N-acyl chain melting can be observed separately [30]. In mixtures containing C16:0 SM and C16:0 Cer at 90:10 mol ratio the onset of the Cer transition occurred at a higher temperature than that of SM, in agreement with our interpretations of the DSC data. This means that, in the coexistence region, the gel phase will be enriched in C16:0 Cer relative to the overall sample composition.

Table 3
Thermodynamic parameters of thermotropic transitions of sphingomyelins with ceramides containing the same N-acyl chain. (SM:Cer 90:10 mol ratio).

N-acyl chain	Components	T_m (°C)	ΔH (Kcal/mol)	WHH (°C)
6		–	–	–
12		18.1	1.88	3.2
	1	15.1	0.24	2.5
	2	18.1	1.61	3.1
	3	46.9	0.26	19.5
	4	61.0	0.29	25.9
16		39.9	8.37	3.6
	1	39.5	18.24	3.0
	2	45.7	4.81	12.1
	3	53.0	1.81	5.0
Egg		37.4	8.13	8.1
	1	37.0	4.08	7.3
	2	46.1	2.72	7.9
	3	50.9	1.10	3.8
18		44.7	6.08	4.5
	1	44.5	1.85	5.6
	2	44.7	0.14	1.3
	3	51.5	3.04	8.5
	4	57.0	1.27	4.5
24		47.3	12.58	16.5
	1	40.7	1.93	7.8
	2	42.5	0.50	2.1
	3	47.0	3.05	5.6
	4	53.1	6.09	12.0
	5	55.9	0.82	4.7
24:1		27.3	4.23	12.6
	1	27.1	2.02	10.7
	2	27.2	0.73	4.9
	3	32.7	1.31	6.7
	4	35.5	0.29	2.7

When the different SM (C6 to C24:1) are mixed with egg ceramide at a 90:10 SM:Cer mol ratio a series of complex endotherms are revealed by DSC (Figs. 1D, S1C–S7C, Table 4). The results can be interpreted in the light of the above observations. In general the transition occurs in the T range of the pure SM, so that the thermograms in Fig. 1C and D are very similar. Westerlund et al. [9] also observed that when C16 SM was mixed with ceramides (C4–C24:1) at a 90:10 SM:Cer mol ratio the endotherm had its main component very close to the T_m of the SM. In our case the main difference is seen with C6 SM mixed with egg Cer (Fig. S1C). Unlike the C6:C6 mixture, that shows no endotherm in the 10–105 °C range, C6:egg displays a complex endotherm with $T_m \approx 33$ °C plus another equally complex signal at ≈94 °C. The data indicate clearly poor mixing of C6 SM and egg Cer, probably due to the very different T_m of both lipids in pure form, respectively <15 °C and 87 °C.

3.5. Sphingomyelins in complex lipid mixtures. Effect of sphingomyelinase

Previous studies from this laboratory [9,27] had shown that when liposomes composed of egg SM, phosphatidylethanolamine (PE) and cholesterol (Chol) in a 2:1:1 mol ratio were treated with a bacterial sphingomyelinase, the subsequent degradation of SM to Cer was accompanied by vesicle aggregation and release of aqueous vesicular contents. A similar study was carried out with SM of different N-acyl chain lengths. Under these conditions SM is the only lipid that can be hydrolyzed by sphingomyelinase. The results are summarized below.

Table 4
Thermodynamic parameters of thermotropic transitions of sphingomyelins with egg ceramide. (SM:Cer 90:10 mol ratio).

N-acyl chain	Components	T_m (°C)		ΔH (Kcal/mol)		WHH (°C)	
6		33.5	93.9	0.640	1.420	4.8	4.4
	1		29.2		0.40		7.0
	2		33.6		0.24		3.2
	3		90.0		0.09		2.0
	4		94.2		1.19		4.5
	5		101.1		0.14		2.8
12		17.6		1.55		6.0	
	1		17.6		1.00		5.7
	2		23.3		0.27		3.8
	3		42.2		0.21		41.4
	4		55.3		0.10		38.4
	5		61.5		0.28		19.8
16		40.6		8.52		2.6	
	1		40.4		1.98		2.1
	2		44.9		4.01		7.9
	3		52.1		2.57		5.3
Egg		37.4		8.13		8.1	
	1		37.0		4.08		7.3
	2		46.1		2.72		7.9
	3		50.9		1.10		3.8
18		44.7		6.33		6.1	
	1		44.4		1.71		4.7
	2		51.3		3.27		8.9
	3		57.0		1.37		4.7
24		48.5		7.26		7.8	
	1		40.7		0.56		1.4
	2		48.5		3.22		4.5
	3		53.1		3.17		6.8
24:1		26.6		3.11		7.5	
	1		17.6		1.06		5.7
	2		23.5		0.29		3.8
	3		38.1		0.50		41.4
	4		52.5		0.46		38.4
	5		59.8		0.21		19.8

With all samples enzyme addition is followed almost immediately (lag time < 3 s) by a rapid increase in turbidity, measured as absorbance at 400 nm. The change in turbidity parallels the initial burst of enzyme activity [12,31]. Representative time courses of turbidity changes are shown in Fig. 3A. In some cases, e.g. with C16:0 and C18:0 SM the particles reach a size such that the "Rayleigh condition" does not hold, i.e. that turbidity no longer increases, and it actually decreases, with particle size [32]. The rates of increase in turbidity are summarized in Fig. 3C. SM with short (C6:0, C12:0) or unsaturated (egg, C18:1, C24:1) N-acyl chains are hydrolyzed at faster initial rates.

Efflux of vesicular aqueous contents is a phenomenon secondary to SM hydrolysis and ceramide formation [12–14]. Representative traces of the time-courses of sphingomyelinase-induced release of contents are shown in Fig. 3B, and the corresponding initial rates are plotted in Fig. 3D. No efflux results could be obtained from LUV containing C24:0 SM because the vesicles were inherently leaky, presumably due to gel–fluid domain coexistence. Among the remaining samples, there is no obvious correlation between the rates of SM hydrolysis (turbidity) and the rates of vesicle efflux. Release is notoriously faster with the C18:0 and C18:1 ceramides, although no obvious explanation can be offered for this behavior.

The higher rate of SM hydrolysis and vesicle aggregation for the short and unsaturated N-acyl chain sphingomyelins (Fig. 3C) could be related to the fluidity of the SM:PE:Chol bilayers. To test this possibility, the various samples studied in Fig. 3 were also examined by differential scanning calorimetry (Fig. 4). In general, whenever thermotropic transitions were found, they were extremely wide. This is expected from the known thermotropic behavior of SM when mixed with other phospholipids and/or cholesterol [33,34]. Mixtures with SM containing C6:0 and C12:0 showed no endotherm signals. The sample with egg SM exhibited a very wide endotherm centered at 30.7 °C. The composition with C24:1 SM had a T_m at 23 °C, and those with C16:0, C18:0 and C24:0 SM showed transitions with midpoints at 36.8 °C, 36.1 °C and 41.2 °C respectively. Since the enzyme assays were performed at 37 °C, it is clear that faster enzyme-dependent aggregation rates were found when the bilayer was more fluid, thus explaining the results in Fig. 3C. This would be against the prediction that the enzyme activity should be favored by the structural defects present during the broad phase transition.

The detection of thermotropic transitions in the mixtures could be due to the presence of observable domains in the bilayers. GUV were made with the different lipid compositions used in Fig. 4, but the vesicles appeared homogeneous under the confocal microscope at 37 °C. (Fig. S9), suggesting that the observed wide transition had its origin in the melting of multiple micro-domains, which in turn would explain the low cooperativity (wide transitions).

4. Discussion

4.1. Pure SM and Cer

A comparative study as attempted in this contribution must inevitably lead to an analysis of similitudes and differences of the objects compared, sphingolipids in the present cases. Similarities are easy to detect. Among sphingomyelins: (i) all SM tested formed bilayers and vesicles in aqueous media, either pure or in mixtures with PE and Chol, (ii) all of them, within the experimental range of our instruments, exhibited gel–fluid transitions whose T_m and enthalpies increased with N-acyl chain length, (iii) N-acyl chain unsaturation led to a lower T_m, as in the case of other phospholipids. For ceramides, (i) all of them, from C12:0 onwards were highly nonpolar and difficult to disperse in water, (ii) all of them displayed narrow rigid–fluid thermotropic transitions, whose temperatures increased with N-acyl chain length and decreased with N-acyl unsaturation. In general the thermotropic properties of SM and Cer follow the patterns of the glycerophospholipids.

Examining the peculiarities of these lipids is more interesting. The SM, being each of them chemically defined, pure compounds, has a complex thermotropic behavior. Multiple endotherms are often found (C18:0, C24:0) and even within each endotherm several components are readily distinguished resulting in asymmetric shapes. For C18:0 SM an intermediate state is attained at ~40 °C when at least two well-defined phases coexist (Fig. 2). We have described the two phases as 'gel' and 'interdigitated gel', following the studies by Guler et al. [35] on dihexadecylphosphatidylcholine, but similar observations in related systems have been attributed to rippled and straight gel phases [36], or gel and fluid phases [37]. The fact that the simplest endotherm is found for the C16:0 SM, i.e. when lipid alkyl chain asymmetry is lowest, suggests that at least part of the thermal complexity is due to the coexistence of domains with different degrees of partial interdigitation. Studies on glycerophospholipids with asymmetric chain lengths have been performed [38–40] but the observed behavior is not as complex as in our case. On the basis of the available data sphingomyelins are, if not unique, at least a rare example of single chemical species of lipids that adopt heterogeneous organizations in water. It should be noted in this context that the thermograms shown in Fig. 1 are third scans, and that further scanning, that was systematically tested, did not change the endotherm line shape.

With respect to ceramide thermal properties, two kinds of irregularities are observed, namely the appearance of minor endotherms, and the presence of exotherms. Minor endotherms, representing < 15% of the total heat absorption, occur with C18:0 and with C24:1 ceramides but not e.g. with C24:0 (Table 2). The presence of exotherms only in the C12:0, C18:0 and C24:0 also fails to adopt a recognizable pattern. The proposed origin of exotherms, i.e. metastable crystalline states [27], does not give reason of the a priori unpredictable thermotropic behavior

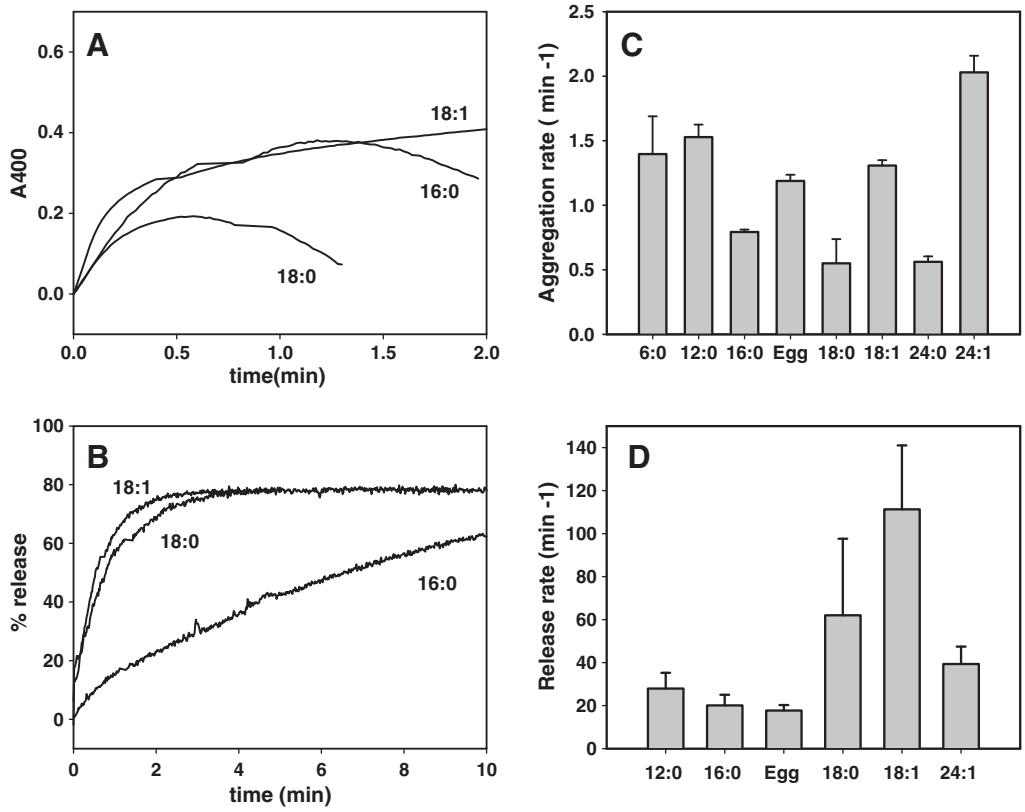

Fig. 3. Sphingomyelinase activities on SM with different N-acyl chains. In all cases the bilayers consisted initially of SM:PE:Chol (2:1:1 mol ratio). (A) Examples of time courses of sphingomyelinase-induced vesicle aggregation, measured as an increase in suspension turbidity (A_{400}). (B) Examples of time-courses of sphingomyelinase-induced release of vesicular aqueous contents. (C) Aggregation rates as a function of N-acyl chain length. (D) Release (efflux) rates as a function of N-acyl chain length. In C and D "rates" refer to initial rates measured respectively as absorbance and fluorescence units/time. Average values ± S.E.M. (n = 3).

of a given ceramide. As mentioned above in relation to C24:1 Cer, the sample thermal history may influence considerably the calorimetric measurements. This is why our C24:1 Cer results may not be directly comparable with those from Pinto et al. [8], but are consistent within our study. In the context of Cer behaviour recent studies by Maggio and co-workers [41,42] have described the complex properties of chain length-mismatched ceramide mixtures and even of some pure ceramides in monolayers.

4.2. SM in mixtures

It is somewhat paradoxical that SM:Cer mixtures, at least at the 90:10 ratios behave in a more predictable way than any of their ingredients. The endotherms contain roughly components corresponding to SM-rich and to Cer-rich domains. It appears as if the increased entropy that is inherent to mixing has destroyed the local micro-organizations that rendered the pure SM and pure Cer thermograms so complex.

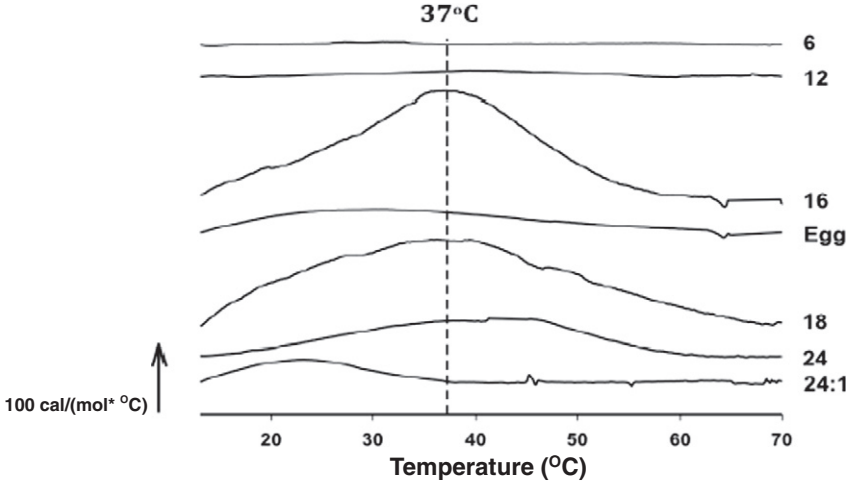

Fig. 4. DSC thermograms of SM:PE:Chol mixtures containing SM with different N-acyl chains. Chain-lengths are indicated at the right-hand side of each curve. The vertical line at 37 °C indicates the temperature at which the sphingomyelinase assays were performed. Representative results (3rd scans) of two closely similar measurements.

The experiments with SM:PE:Chol bilayers and sphingomyelinase represent a higher degree of complexity, since the enzyme is progressively degrading SM to yield Cer. Quantitative estimates of SM disappearance indicate that roughly 20% SM is degraded in the first minute under our conditions, but hydrolysis is not likely to proceed linearly with time. Thus in the experiments shown in Fig. 3 and in particular at the initial stages when initial rates are measured, SM and Cer are coexisting in the bilayers, mimicking the situation in the plasma membranes when SM is being hydrolyzed in response to a stress signal [3,4]. In these mixtures the hydrolysis rate appears to be higher for lipids in the fluid phase (Fig. 3C), in agreement with previous data [28]. Ceramide is known to break down the permeability barrier of lipid bilayers [13,14,31]. This is indeed observed with all SM tested, however for reasons that are not known at present, leakage was much faster in the mixtures containing C18:0 and C18:1 SM (Fig. 3D). Contents release was in all cases 60–80% of total when a steady-state was reached (data not shown). The mechanism of Cer-induced vesicle efflux is not fully understood yet, and this makes more difficult interpreting the leakage data in Fig. 3D.

4.3. Many ceramides, many sphingolipids

Hannun and Obeid [1] have proposed the "many ceramides" paradigm (analogous to the "many worlds" interpretation of quantum mechanics) to emphasize the amazing complexity of a group of seemingly simple molecules functionally neglected until recently, and presumed to be structurally thus physically homogeneous. The data in this paper support the notion that ceramides are actually complex not only from the point of view of their biological effects, but also when their thermal properties are considered. Some basic aspects e.g. the number and sign of endotherms, cannot be immediately deduced from the structure. Their membrane-permeabilizing properties also vary in a complex way with chain length/unsaturation.

SM are structurally based on Cer, with an additional phosphorylcholine polar moiety. If each individual Cer has its own, sometimes unexpected properties, the same can be said of SM, particularly in what refers to their capacity (e.g. C18:0 SM) to adopt two coexisting bilayer organizations. Thus many SM as well, again with properties that vary non-linearly with structure. Interestingly, SM:Cer mixtures show thermotropic properties that are somewhat predictable from the properties of the pure compounds. Maybe this is just a step in the process of achieving a rather uniform set of biological membranes from highly heterologous constituents.

A final word on heterogeneity concerns the very different and often unexpected membrane properties of the "simple sphingolipids", sphingosine, ceramide, and their phosphorylated forms [2]. Ceramide and sphingosine increase markedly membrane permeability; ceramide, but not sphingosine, induce transbilayer phospholipid motion (flip–flop); ceramide-1-phosphate is alone in this group to form bilayers; sphingosine-1-phosphate has a marked affinity for water, and so on. There are virtually no data on of the N-acyl chain effect on these properties. Many sphingolipids exhibit many remarkable physical properties. Many of these physical data have not yet found a physiological or pathological correlate. Paraphrasing Hannun and Obeid [1] the study of even the simplest of sphingolipids is unfolding into a world of their own, a world of enigmas and unique promise.

Acknowledgments

This work was supported in part by grants from the Spanish Ministerio de Economía (BFU 2007-62062; BFU 2011-28566) and the Basque Government (IT838-13; IT849-13). N.J.R. and A.B.G.A. were pre-doctoral students supported by the Basque Government.

Appendix A. Supplementary data

Supplementary data to this article can be found online at http://dx.doi.org/10.1016/j.bbamem.2013.10.010.

References

[1] Y.A. Hannun, L.M. Obeid, Many ceramides, J. Biol. Chem. 286 (32) (Aug 12 2011) 27855–27862.
[2] F.M. Goñi, A. Alonso, Biophysics of sphingolipids I. Membrane properties of sphingosine, ceramides and other simple sphingolipids, Biochim. Biophys. Acta 1758 (12) (Dec 2006) 1902–1921.
[3] A.E. Cremesti, F.M. Goni, R. Kolesnick, Role of sphingomyelinase and ceramide in modulating rafts: do biophysical properties determine biologic outcome? FEBS Lett. 531 (1) (Oct 30 2002) 47–53.
[4] R.N. Kolesnick, F.M. Goñi, A. Alonso, Compartmentalization of ceramide signaling: physical foundations and biological effects, J. Cell. Physiol. 184 (3) (Sep 2000) 285–300.
[5] T. Maula, I. Artetxe, P.M. Grandell, J.P. Slotte, Importance of the sphingoid base length for the membrane properties of ceramides, Biophys. J. 103 (9) (Nov 7 2012) 1870–1879.
[6] I. Artetxe, C. Sergelius, M. Kurita, S. Yamaguchi, S. Katsumura, J.P. Slotte, T. Maula, Effects of sphingomyelin headgroup size on interactions with ceramide, Biophys. J. 104 (3) (Feb 5 2013) 604–612.
[7] S.N. Pinto, L.C. Silva, R.F. de Almeida, M. Prieto, Membrane domain formation, interdigitation, and morphological alterations induced by the very long chain asymmetric C24:1 ceramide, Biophys. J. 95 (6) (Sep 15 2008) 2867–2879.
[8] S.N. Pinto, L.C. Silva, A.H. Futerman, M. Prieto, Effect of ceramide structure on membrane biophysical properties: the role of acyl chain length and unsaturation, Biochim. Biophys. Acta 1808 (11) (Nov 2011) 2753–2760.
[9] B. Westerlund, P.M. Grandell, Y.J. Isaksson, J.P. Slotte, Ceramide acyl chain length markedly influences miscibility with palmitoyl sphingomyelin in bilayer membranes, Eur. Biophys. J. 39 (8) (Jul 2010) 1117–1128.
[10] J. Sot, L.A. Bagatolli, F.M. Goñi, A. Alonso, Detergent-resistant, ceramide-enriched domains in sphingomyelin/ceramide bilayers, Biophys. J. 90 (3) (Feb 1 2006) 903–914.
[11] J.V. Busto, M.L. Fanani, L. De Tullio, J. Sot, B. Maggio, F.M. Goñi, A. Alonso, Coexistence of immiscible mixtures of palmitoylsphingomyelin and palmitoylceramide in monolayers and bilayers, Biophys. J. 97 (10) (Nov 18 2009) 2717–2726.
[12] F.M. Goñi, L.R. Montes, A. Alonso, Phospholipases C and sphingomyelinases: lipids as substrates and modulators of enzyme activity, Prog. Lipid Res. 51 (3) (Jul 2012) 238–266.
[13] M.B. Ruiz-Argüello, G. Basáñez, F.M. Goñi, A. Alonso, Different effects of enzyme-generated ceramides and diacylglycerols in phospholipid membrane fusion and leakage, J. Biol. Chem. 271 (43) (Oct 25 1996) 26616–26621.
[14] L.R. Montes, M.B. Ruiz-Argüello, F.M. Goñi, A. Alonso, Membrane restructuring via ceramide results in enhanced solute efflux, J. Biol. Chem. 277 (14) (Apr 5 2002) 11788–11794.
[15] H.M. McConnell, T.H. Watts, R.M. Weis, A.A. Brian, Supported planar membranes in studies of cell–cell recognition in the immune system, Biochim. Biophys. Acta 864 (1986) 95–106.
[16] Gr Bartlett, Phosphorus assay in column chromatography, J. Biol. Chem. 234 (3) (Mar 1959) 466–468.
[17] H. Ellens, J. Bentz, F.C. Szoka, Destabilization of phosphatidylethanolamine liposomes at the hexagonal phase transition temperature, Biochemistry 25 (2) (Jan 28 1986) 285–294.
[18] F.M. Goñi, A.V. Villar, J.L. Nieva, A. Alonso, Interaction of phospholipases C and sphingomyelinase with liposomes, Methods Enzymol. 372 (2003) 3–19.
[19] J.L. Nieva, F.M. Goñi, A. Alonso, Liposome fusion catalytically induced by phospholipase C, Biochemistry 28 (18) (Sep 5 1989) 7364–7367.
[20] P.R. Maulik, G.G. Shipley, N-palmitoyl sphingomyelin bilayers: structure and interactions with cholesterol and dipalmitoylphosphatidylcholine, Biochemistry 35 (24) (Jun 18 1996) 8025–8034.
[21] Y.J. Björkqvist, J. Brewer, L.A. Bagatolli, J.P. Slotte, B. Westerlund, Thermotropic behavior and lateral distribution of very long chain sphingolipids, Biochim. Biophys. Acta 1788 (6) (Jun 2009) 1310–1320.
[22] X.M. Li, J.M. Smaby, M.M. Momsen, H.L. Brockman, R.E. Brown, Sphingomyelin interfacial behavior: the impact of changing acyl chain composition, Biophys. J. 78 (4) (Apr 2000) 1921–1931.
[23] T.Y. Ahmad, J.T. Sparrow, J.D. Morrisett, Fluorine-, pyrene-, and nitroxide-labeled sphingomyelin: semi-synthesis and thermotropic properties, J. Lipid Res. 26 (9) (Sep 1985) 1160–1165.
[24] T.J. McIntosh, S.A. Simon, D. Needham, C.H. Huang, Structure and cohesive properties of sphingomyelin/cholesterol bilayers, Biochemistry 31 (7) (Feb 25 1992) 2012–2020.
[25] B. Gaigg, A. Toulmay, R. Schneiter, Very long-chain fatty acid-containing lipids rather than sphingolipids per se are required for raft association and stable surface transport of newly synthesized plasma membrane ATPase in yeast, J. Biol. Chem. 281 (45) (Nov 10 2006) 34135–34145.
[26] K. Iwabuchi, A. Prinetti, S. Sonnino, L. Mauri, T. Kobayashi, K. Ishii, N. Kaga, K. Murayama, H. Kurihara, H. Nakayama, F. Yoshizaki, K. Takamori, H. Ogawa, I. Nagaoka, Involvement of very long fatty acid-containing lactosylceramide in lactosylceramide-mediated superoxide generation and migration in neutrophils, Glycoconj. J. 25 (4) (May 2008) 357–374.
[27] J. Shah, J.M. Atienza, R.I. Duclos Jr., A.V. Rawlings, Z. Dong, G.G. Shipley, Structural and thermotropic properties of synthetic C16:0 (palmitoyl) ceramide: effect of hydration, J. Lipid Res. 36 (9) (Sep 1995) 1936–1944.

[28] B. Maggio, T. Ariga, J.M. Sturtevant, R.K. Yu, Thermotropic behavior of glycosphingolipids in aqueous dispersions, Biochemistry 24 (5) (Feb 26 1985) 1084–1092.
[29] M.P. Veiga, J.L. Arrondo, F.M. Goñi, A. Alonso, Ceramides in phospholipid membranes: effects on bilayer stability and transition to nonlamellar phases, Biophys. J. 76 (1 Pt 1) (Jan 1999) 342–350.
[30] S.S. Leung, J.V. Busto, A. Keyvanloo, F.M. Goñi, J. Thewalt, Insights into sphingolipid miscibility: separate observation of sphingomyelin and ceramide N-acyl chain melting, Biophys. J. 103 (12) (Dec 19 2012) 2465–2474.
[31] M.B. Ruiz-Argüello, F.M. Goñi, A. Alonso, Vesicle membrane fusion induced by the concerted activities of sphingomyelinase and phospholipase C, J. Biol. Chem. 273 (36) (Sep 4 1998) 22977–22982.
[32] A.-R. Viguera, A. Alonso, F.M. Goñi, Liposome aggregation induced by poly(ethylene glycol). Rapid kinetic studies, Colloids Surf. B 3 (1995) 263–270.
[33] M.B. Ruiz-Argüello, M.P. Veiga, J.L. Arrondo, F.M. Goñi, A. Alonso, Sphingomyelinase cleavage of sphingomyelin in pure and mixed lipid membranes. Influence of the physical state of the sphingolipid, Chem. Phys. Lipids 114 (1) (Jan 2002) 11–20.
[34] F.X. Contreras, J. Sot, M.B. Ruiz-Argüello, A. Alonso, F.M. Goñi, Cholesterol modulation of sphingomyelinase activity at physiological temperatures, Chem. Phys. Lipids 130 (2) (Jul 2004) 127–134.
[35] S.D. Guler, D.D. Ghosh, J.J. Pan, J.C. Mathai, M.L. Zeidel, J.F. Nagle, S. Tristram-Nagle, Effects of ether vs. ester linkage on lipid bilayer structure and water permeability, Chem. Phys. Lipids 160 (2009) 33–44.
[36] H. Takahashi, T. Hayakawa, Y. Kawasaki, K. Ito, T. Fujisawa, M. Kodama, T. Kobayashi, Structural characterization of N-lignoceroyl (C24:0) sphingomyelin bilayer membranes: a re-evaluation, J. Appl. Crystallogr. 40 (2007) s312–s317.
[37] R.N.A.H. Lewis, R.N. McElhaney, F. Österberg, S.M. Gruner, Enigmatic thermotropic phase behaviour of highly asymmetric mixed-chain phosphatidylcholines that form mixed-interdigitated gel phases, Biophys. J. 66 (1994) 207–216.
[38] C. Huang, J.T. Mason, Structure and properties of mixed-chain phospholipid assemblies, Biochim. Biophys. Acta Rev. Biomembr. 864 (1986) 423–470.
[39] M. Goto, S. Ishida, N. Tamai, H. Matsuki, S. Kaneshina, Chain asymmetry alters thermotropic and barotropic properties of phospholipid bilayer membranes, Chem. Phys. Lipids 161 (2009) 65–76.
[40] D. Marsh, Handbook of lipid bilayers, 2nd ed. CRC Press, Boca Raton, USA, 2013.
[41] F. Dupuy, B. Maggio, The hydrophobic mismatch determines the miscibility of ceramides in lipid monolayers, Chem. Phys. Lipids 165 (2012) 615–629.
[42] M.L. Fanani, B. Maggio, Phase state and surface topography of palmitoyl-ceramide monolayers, Chem Phys Lipids 163 (2010) 594–600.